Published by Avanti Publishers

Journal of Advanced Thermal Science Research

ISSN (online): 2409-5826


# Comparison Study of Cascaded Organic Rankine Cycles with Single and Dual Working Fluids for Waste Heat Recovery

Gerutu B. Gerutu [1] and Yossapong Laoonual [2,3,*]

[1]*The Joint Graduate School of Energy and Environment,* [2]*Mobility & Vehicle Technology Research Center (MOVE),* [3]*Department of Mechanical Engineering, Faculty of Engineering, King Mongkut's University of Technology Thonburi, 126 Pracha Uthit Road, Bang Mod, Thung Kru, Bangkok 10140, Thailand*

## ARTICLE INFO

*Article Type*: Research Article

*Academic Editor*: Xiaohui Yu

*Keywords*:
Working fluids
Cascaded ORC
Environmental saving
Thermal performance
Economic performance

*Timeline*:
Received: April 03, 2024
Accepted: May 06, 2024
Published: May 24, 2024

*Citation*: Gerutu GB, Laoonual Y. Comparison study of cascaded organic rankine cycles with single and dual working fluids for waste heat recovery. J Adv Therm Sci Res. 2024; 11: 1-21.

*DOI*: https://doi.org/10.15377/2409-5826.2024.11.1

## ABSTRACT

This study compares thermodynamics, economics, and environmental performance of cascaded ORCs operated under a single and dual fluids. In the single fluid cascaded ORC, toluene, benzene, acetone and cyclopentane are run in high and low temperature cycles, whereas in dual fluid cascaded ORC, toluene, benzene, acetone and cyclopentane are run in high temperature cycle and R601a in the low temperature cycle. The analysis compares variations in expander inlet temperature and condensation temperature. Thermodynamic performance involved net power output ($P_{net}$) and thermal efficiency ($\eta_{th}$), while economic indicators included net present value (NPV) and levelized cost of electricity (LCOE). In environmental performance, the annual reduction in carbon dioxide emission ($CO_{2\text{-}eq}$) is assessed. The findings revealed that dual fluid cascaded ORC generated the highest $P_{net}$ of 1245.11 kW while single fluid cascaded ORC reached 1170.27 kW. The dual fluid cascaded ORC showed the significant increase in $P_{net}$ ($\%\Delta P_{net}$) for about 43% at the lowest expander inlet temperature (500 K). In terms of $\eta_{th}$, dual fluid cascaded ORC attained 37.23 % while single fluid cascaded ORC reached 33.25%. It is further found that acetone+R601a performed well in dual fluid cascaded ORC, resulting in the highest $P_{net}$ and allowing system's NPV to turn positive sooner than other fluids. Furthermore, cyclopentane+R601a had the lowest LCOE of 0.0158 US$/kWh, which is 1.1% lower compared to the single fluid cascaded ORC and competitive in the Thai electricity market. In environmental saving, dual fluid cascaded ORC reduced about 144.96 $tCO_{2\text{-}eq}$/year, and outperformed single fluid cascaded ORC by roughly 6.39%.

*Corresponding Author
Email: yossapong.lao@kmutt.ac.th
Tel: +(66) 092 456 8936

# 1. Introduction

Increased global energy demand [1-3] has resulted in energy and environmental crises [4], resulting in global warming [5, 6] and extreme weather changes [7]. Since fossil fuels are still the main source of energy used to generate electricity, more than half of the primary energy is wasted [8] and released into the environment [4, 9-18]. In the waste energy discharged into the environment, carbon dioxide ($CO_2$) dominates the emissions, causing a major concern [1, 3] and is accountable for a number of extreme weather events [7]. Globally, $CO_2$ emissions are increasing annually and have surpassed 3.712 trillion tons in 2021 [19, 20]. Consequently, countries are under growing pressure to pursue lower-carbon development paths due to concerns about environmental pollution, particularly $CO_2$ emissions. In order to reach "carbon neutrality," cutting emissions and improving energy efficiency have emerged as long-term goals.

The organic Rankine cycle (ORC) is a cutting-edge technology that transforms low-grade heat into power via the work of organic working fluids [7]. The technology has gained recognition recently [21] for being suitable, efficient, and clean, with the ability to operate at lower, medium, and higher temperatures. A number of encouraging features are provided by the ORC, such as its simple design, widely accessible equipment, affordable investment costs, and advantageous economics [22-24]. These elements support ORC's attractiveness as an environmentally friendly waste heat recovery solution.

Numerous studies [21, 25, 26] have been carried out recently to evaluate the efficiency of various organic Rankine cycle (ORC) configurations for the production of electricity from waste heat sources. In order to determine the best possible system performance, these studies have highlighted the importance of fluid temperature, cycle configuration, and heat source temperature [21, 26]. The thermodynamic performance of various ORC cycle configuration, including basic ORC (BORC) [21, 27, 28], ORC with recuperator (RORC) [29], and so on, has been investigated using a variety of working fluids and heat source inlet temperatures. However, the BORC has been reported to have a limited thermal efficiency. For instance, Scaccabarozzi *et al*. [28] reported the thermal efficiencies of up to 19.90 % at lower exhaust temperatures (518 K) and up to 23.76% at higher exhaust temperatures (618 K) using various working fluids. There are major performance limitations with current single stage ORC technology as a result of its maximum working fluid operating temperature (about 573 K) [30]. This reduces the amount of heat that the ORC can extract from the waste heat source. Furthermore, variations in the heat source parameters can affect ORC performance and possibly result in system failures [31].

As a substitute strategy for enhancing a single stage ORC performance, a great deal of research has been done on the two-stage ORC for waste heat to power generation, which has been the subject of substantial research to date [31, 32]. The two-stage ORC is made up of two cycles: the high-temperature cycle, which collects temperature from the high heat zone, and the low-temperature cycle, which collects temperature from the low heat zone. Depending on how the heat sources are arranged on the cycles, the two-stage ORC may be in series or cascaded mode. In the cascaded mode, the high-temperature cycle captures heat from the heat source, while the low-temperature cycle extracts heat from the expander outlet of the high-temperature cycle. In the study of Rashwan, Dincer and Mohany [32], compare the basic ORC (BORC), cascade ORC, and recuperator ORC were all tested at 723 K using propane as the working fluid and found that the cascade ORC performed better than the BORC, increasing net power output by 73% and improving thermal efficiency by 8%. White *et al*. [1] reported an 11.1% increase in net power output and a 9.5% improvement in thermal efficiency for the cascade ORC operating at 573 K compared to a single stage ORC. Manente, Lazzaretto and Bonamico [33] found that dual-pressure cascaded systems can produce 20% more net power output than a single-stage ORC. The studies mentioned above demonstrated significant improvements in the performance of the cascaded ORC including the ability to operate at high-temperature heat sources, generating higher net power output and efficiency compared to single stage ORC. However, in these cascaded ORCs only a single fluid is used and thus issues around high-pressure ratios and sub-atmospheric pressures are not addressed [29]. Indeed, despite its importance, the comparison of cascaded ORCs with single and dual fluids is rarely discussed in the literature [33]. Furthermore, studies have focused on the thermodynamic and economic performance of cascaded ORCs while ignoring the environmental aspect, which is critical for dictating a sustainable system. This is a potentially significant factor that should be taken into account in any future techno-economic analysis.

The novelty of this study lies on the comparison of cascaded ORCs with a single and dual working fluid. Furthermore, emphasis is exploring cascaded ORCs for relatively high-temperature applications, where performance gains are expected to be higher, but have not been thoroughly investigated too far. The novelty of is study lies on the comparison base on the thermo-economic and environmental performance which, to the authors' knowledge, allows a more accurate and rigorous comparison than previously conducted. The contributions of the present study include:

- For a single fluid cascaded ORC, toluene, benzene, acetone, and cyclopentane are employed in both high- and low-temperature cycles. In a dual fluid cascaded ORC, the high-temperature cycle utilizes hydrocarbon working fluids (toluene, benzene, acetone, and cyclopentane), while the low-temperature cycle employs R601a refrigerant due to its low ozone depletion potential (ODP), global warming potential (GWP), and net boiling point temperature.
- For gaining the understanding on their performance, cycles are subjected under variations in expander inlet temperature ($T_{exp}$), and condensation temperature ($T_{cond}$).
- Two important thermodynamic performance indicators are analyzed: net power ($P_{net}$) and thermal efficiency ($\eta_{th}$). The goal is to determine the best working fluid and operating condition that will yield the maximum $P_{net}$ and $\eta_{th}$.
- In terms of economic performance, the key indicators are net present value (NPV) and levelized cost of electricity (LCOE). To achieve the best NPV and LCOE, the best working fluid and operating conditions must be identified.
- In environmental savings, the study quantifies the amount of carbon dioxide offset by introducing single and dual fluid cascaded ORCs.
- Lastly, a comparison of cascaded ORCs with single and dual working fluids under various operating situations is made in terms of thermodynamic, economic, and environmental performance.

# 2. Cascaded ORC System Description

## 2.1. Waste Heat Source

A Siemens SGT-400 engine having power generation capacity of 12.90 MWe rating with hybrid combustion system and heat rate of 10,355 kJ/kWh is used in this study. This industrial gas turbine generates an exhaust gas flow of 39.4 kg/s at 555 °C is deployed as the waste heat source. The gas turbine has been selected as among the most practical and economical prime movers for equipment in off-shore platforms. Besides, its turbine technology offers broad fuel flexibility and outstanding efficiencies for economic fuel consumption. The technical specifications of Siemens SGT 400 are shown in Table **1**.

**Table 1: Technical specification for Siemens gas turbine 400.**

| Model | Siemens SGT 400 |
|---|---|
| Turbine inlet temperature | 1,083 K |
| Exhaust gas temperature | 828 K |
| Exhaust gas mass flow | 39.4 kg/s |
| Electrical power output | 12.90 MW (e) |
| Thermal efficiency | 34.8% |
| Fuel | Natural gas |

## 2.2. Cycle Configuration

The cycle configuration of the cascaded ORC and its T-s diagram are shown in Fig. (**1**). The cycle configuration of the cascaded ORC comprises of a high-temperature (cycle 1) and low-temperature (cycle 2) cycles to recover the waste heat from the exhaust gas. Each cycle consists of pump (P), heat exchanger (HEX), expander (EXP), condenser (C) and working fluid. In the high-temperature cycle, a portion of working fluid is compressed by pump 1 ($P_1$) to higher pressure in order to reach a high evaporating temperature that corresponds with the exhaust temperature.

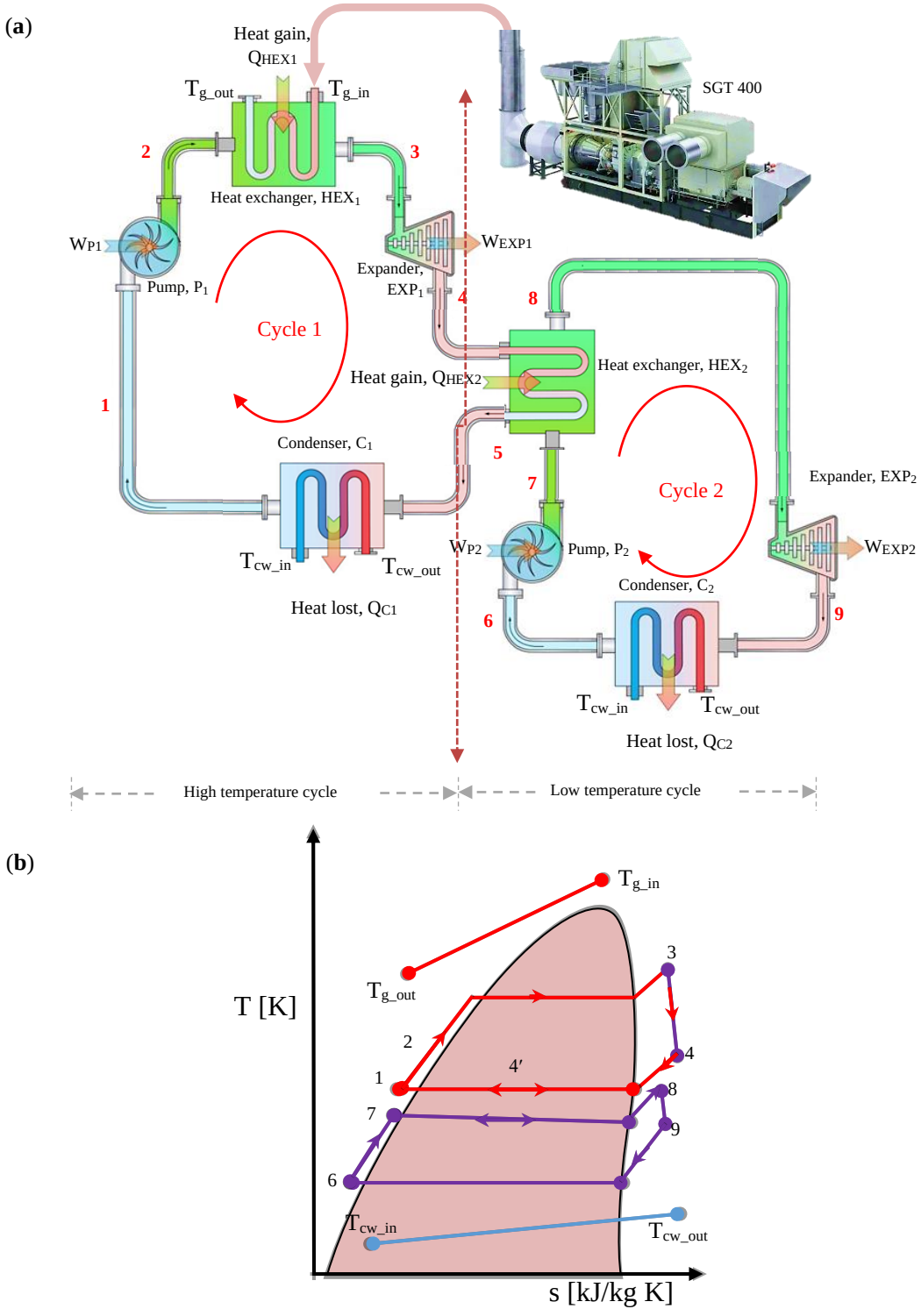


**Figure 1:** Schematic diagram of (**a**) cascaded ORC and (**b**) T-s diagrams of a cascaded ORC.

Then, the pressurized fluid after gaining heat at heat exchanger 1 ($HEX_1$) flows to the expander 1 ($EXP_1$) to perform the useful work and remaining heat after expansion is used as the heat source for expander 2 ($EXP_2$) which is captured by the working fluid compressed by pump 2 ($P_2$). In the low-temperature cycle (cycle 2), the portion part of the working fluid is pressurized to absorb sufficient amount of the heat energy and evaporates to saturated vapor phase state in the heat exchanger 2 ($HEX_2$). After that the low-pressure vapors flow into the condensers 1 ($C_1$) and 2 ($C_2$) and are condensed into saturated liquid phase state. The low-pressure saturated liquid available at the condenser outlets ($C_1$ and $C_2$) are pressurized by the pumps ($P_1$ and $P_2$) and new cycles begin.

## 2.3. Thermodynamic Analysis

The thermodynamic model of the cascaded ORC system is developed, and the pressure drop is taken into consideration. Working fluid side pressure drop of the condenser has a negative effect on system performance because it will influence turbine expansion ratio and pump pressure ratio. This effect will become more significant when condensing pressure lowers. Under the same condensing temperature, the working fluid with high critical temperature usually has a lower condensing pressure. In order to develop suitably mathematical model of the system, the assumptions for the simulation which is based on account of the first law of thermodynamic is carried out as follows:

where $W_P$, $m_{wf}$, $h$ and $\eta_p$ stand for work done by the pump, mass flowrate of the working fluid, specific enthalpy of the fluid stream and isentropic pump efficiency, $\dot{Q}_{HEX}$ stands for the heat gained by the working fluid, the subscripts ext.-g, g_in-1 and g_out-1 express the exhaust gas and exhaust gas at the inlet and outlet of HEX, $W$ and $Q$ represents the work and heat added, the subscripts *net* and *th* mean net and thermal, respectively.

Since the cascaded ORC systems with single and dual working fluids have the same base thermodynamic processes, the energy balance equations of their components and the system efficiency equation based on the first law of thermodynamics can be expressed in a unified form as listed in Table **2**. The mass flow rate and the thermodynamic states of these equations can be calculated by the pinch point temperature difference (PPTD) method [22]. Their calculation programs are achieved in the MS. Excel environment.

**Table 2: Thermodynamic evaluation equations.**

| Cycle | Equipment | Model Equation | Equation Number |
|---|---|---|---|
| High-temperature cycle | Pump 1 | $W_{P1} = \frac{\dot{m}_{wf}(h_2 - h_1) = \dot{m}_{wf}(h_{2s} - h_1)}{\eta_{P1}}$ | 1 |
| | Heat exchanger 1 | $\dot{Q}_{HEX1} = \dot{m}_{wf}(h_3 - h_2) = \dot{m}_{ext,g}(h_{g\_in-1} - h_{g\_out-1})$ | 2 |
| | Expander 1 | $W_{EXP1} = \dot{m}_{wf}(h_3 - h_4) = \dot{m}_{wf}(h_3 - h_{4s}) \times \eta_{EXP1}$ | 3 |
| | Condenser 1 | $\dot{Q}_{C1} = \dot{m}_{wf}(h_{1'} - h_1) = \dot{m}_{cw}(h_{w\_out-1} - h_{w\_in-1})$ | 4 |
| Low-temperature cycle | Pump 2 | $W_{P2} = \frac{\dot{m}_{wf}(h_8 - h_7) = \dot{m}_{wf}(h_{8s} - h_7)}{\eta_{P2}}$ | 5 |
| | Heat exchanger 2 | $\dot{Q}_{HEX2} = \dot{m}_{wf\_ORC2}(h_5 - h_8)$ | 6 |
| | Expander 2 | $W_{EXP2} = \dot{m}_{wf}(h_5 - h_6) = \dot{m}_{wf}(h_5 - h_{6s}) \times \eta_{EXP2}$ | 7 |
| | Condenser 2 | $\dot{Q}_{C2} = \dot{m}_{wf}(h_6 - h_7) = \dot{m}_{cw}(h_{w\_out-2} - h_{w\_in-2})$ | 8 |
| System | Net heat gain | $\dot{Q}_{net} = \dot{Q}_{HEX1} + \dot{Q}_{HEX2}$ | 9 |
| | Net power output | $p_{net} = \eta_g \times [W_{EXP1} + W_{EXP2} - W_{P1} - W_{P2}]$ | 10 |
| | Thermal efficiency | $\eta_{th} = \frac{\dot{W}_{net}}{\dot{Q}_{net}} \times 100\%$ | 11 |

### *2.3.1. Assumptions*

In this part, the model assumptions are presented for the thermodynamic analysis of the cascaded ORC systems. Regarding the cycles' operating conditions, a few assumptions were made:

- It is assumed that all systems operate under steady-state conditions,
- The analysis disregards the effects of friction losses, including those related to heat losses and pressure drop, within the components of the cycle,
- The analysis does not consider the potential energy (gravitational potential) and kinetic energy associated with the fluid within the cycle components,
- The working fluids at the inlet of the turbine and outlet of the condenser are superheated steam and subcooled liquid respectively, and
- The working fluids entering the fluid pumps are assumed to be in a saturated liquid state.

As a result, by ignoring those elements that are anticipated to have little bearing on the system's overall performance, these assumptions streamline the thermodynamic analysis. The parameters used in the modeling of the cascaded ORC are shown in Table **3**.

**Table 3: Parameters used in the modelling of the cascaded ORC.**

| Parameter | Abbreviation | Unit | Value | References |
|---|---|---|---|---|
| Heat source temperature | $T_{g-in}$ | K | 823 | [34] |
| Mass flow rate of the flue gas | $m_{wf}$ | kg/s | 44 | [ 34] |
| Isentropic pump efficiency | $\eta_P$ | % | 50 | [31] |
| Isentropic expander efficiency | $\eta_{EXP}$ | % | 85 | [32-34] |
| Generator efficiency | $\eta_{gen}$ | % | 98 | [6, 35, 36] |
| Ambient pressure | $P_O$ | MPa | 0.1 | [33, 37] |
| Ambient temperature | $T_O$ | K | 303 | [33] |
| Heat exchanger efficiency | $\eta_{HEX}$ | % | 85 | [27] |
| Pinch point in heat exchanger | $\Delta T_{HEX\,1}$ | K | 20 | [31] |
| Pinch point in heat exchanger | $\Delta T_{HEX\,2}$ | K | 10 | [31] |
| Pinch point in condenser | $\Delta T_C$ | K | 10 | [31] |
| Condenser Temperature | $T_{cw-in}$ | K | 313 | [6] |

## 2.4. Selection of Working Fluids

The choice of a suitable working fluid has been extensively covered in publications and is crucial to the ORC design. To maximize performance in terms of net power output and thermal efficiency, a working fluid pair had to be found for the high-temperature and low-temperature cascade ORC, respectively. These pairs had to match with the heat sink and sources of heat as well as each other. In addition, consideration has to be given to safety aspects like flammability and toxicity [38], environmental variables like the global warming potential (GWP) and ozone depletion potential (ODP), as well as practical and regulatory constraints. In reference to the latter, it was necessary to have a condensation pressure that was close to ambient pressure in order to prevent air leaks into the system [39] and a maximum pressure of 20 bar in order to receive technical certification and make use of common industrial components possible. Furthermore, the normal boiling point temperature (NBPT) of the working fluids should be higher than 25°C. This allowed for the opening of circuits and construction alterations to be made to the experimental setup without having to remove the working fluids.

Regarding the heat source, the choice of possible working fluids for the cascading ORC is determined by taking into account the high and low boiling temperatures that are appropriate for that particular application. Hydrocarbon and refrigerant fluids are the main subject of the current study, whereas high-critical-temperature fluids were selected for high-temperature cycles that operate at high heat sources. Toluene, benzene, cyclopentane, and acetone are these fluids. The zero-ozone depletion and global warming potentials of toluene, benzene, cyclopentane, and acetone are advantageous properties [40], however there were no comparable data for R601a. These results led to the selection of acetone, toluene, benzene, and cyclopentane as working fluids for the high-temperature cycle of cascaded ORC with dual fluids. This was done not only because of the advantageous operational and safety aspects of these fluids, but also because of their higher thermal efficiency and power output. Thus, most of the common working fluids for low temperature applications were ruled out and R601a was considered in the present study. The thermodynamic characteristics of the selected refrigerant fluid and the chosen hydrocarbon fluids are shown in Table **4**. The system is thermodynamically modeled using Microsoft Excel for simulation purposes. The CoolProp version 6.4.1 software provides the thermodynamic characteristics of the working fluids and can be used as a reference to retrieve the necessary fluid properties. Subsequently, the performance of the cascaded ORC with single working fluid is calculated based on the toluene, the best performing fluid. On the other hand, the performance of the cascaded ORC with dual working fluids was calculated for hydrocarbon working fluids in the high-temperature cycle and refrigerant in the low-temperature cycle.

**Table 4: Thermodynamic properties of the selected working fluids.**

| Fluid Name | Molecular Mass (g/mol) | Boiling Point (K) | $T_{cr}$ (K) | $P_{cr}$ (bar) | Thermal Stability Temp (K) | ODP | GWP (100 yrs) | ASHRAE std 34 Safety Class | Slope |
|---|---|---|---|---|---|---|---|---|---|
| Benzene | 78.11 | 353.23 | 835 | 4.89 | 626.2 | 0 | low | - | Dry |
| Cyclopentane | 70.13 | 322.4 | 511.6 | 4.571 | 511.6 | 0 | < 11 | - | Isentropic |
| Toluene | 92.14 | 383.6 | 591.75 | 4.13 | | 0 | 3 | - | Dry |
| Acetone | 58.08 | 329 | 508 | 4.69 | 329 | 0 | low | - | Dry |
| R601a | 72.15 | 300.9 | 460.2 | 33.78 | 300.9 | 0 | low | | |

# 3. Economic Performance

Three crucial factors are used to assess the economic performance of the cascaded ORCs: net present value (NPV) and levelized cost of electricity (LCOE). The NPV technique is provided in Eqn. (12) and was adopted from [7, 32], and [41]. Based on Eqn. (12), $I_{fuel}$ and $I_{CO2}$ are the yearly revenue resulting from fuel and $CO_2$ savings. The $I_{fuel}$ is linked to the energy produced by the cascaded ORC, allowing the industrial gas turbine's load to be reduced. Thus, the fuel that was conserved can later be sold on the market. As a result, there is less fuel burning and $CO_2$ emissions when the strain on natural gas is reduced. In that instance, reducing $CO_2$ recovers the funds that may be used to pay for a carbon. The net present value (NPV) is computed using the yearly revenue from electricity sales, the cost of $CO_2$ savings, and the annual expenses. The $CO_2$ emitted by the industrial gas turbine is computed based on the fuel consumption approach. The $CO_2$ emissions from the cascaded ORC's yearly energy generation can be computed using conversion factors of 0.0133 kg$CO_2$/kWh, 65 g(fuel)/kWh [41], and an electricity cost of 0.122 US$/kWh in Thailand. *Mf* is set to 0.9 [41] to account for maintenance and operation costs. Table **5** lists the parameters used in economic performance.

$$NPV = \sum_{n=1}^{21} \frac{I_{fuel} + I_{CO2}}{(1+i)^n} - M_f TIC \tag{12}$$

Based on data from Pierobon *et al*. [41], 7 % and 20 years, respectively, are suitable values for discount rate (*i*) and project lifetime (*n*). The total cost of investment (TIC), as indicated in Table **3**, comprises component costs in addition to other expenses. The cost correlations used to calculate the cascaded ORC component purchasing cost are displayed in Table **6**.

**Table 5: Parameters used in economic modelling [7].**

| Total Capital Investment (TIC) | I +II |
|---|---|
| I. Fixed capital investment (FCI) | DC + IC |
| A. Direct cost (DC) | |
| Purchased equipment costs (PEC) | 15% PEC |
| Purchased equipment installation piping | 35% PEC |
| Instrumentational and controls | 12% PEC |
| Electrical equipment and materials | 13% PEC |
| B. Indirect cost | |
| a) Engineering and supervision | 4% DC |
| b) Construction costs and contractor's profit | 15% DC |
| Contingencies | 10% of (a &b) |
| II. Others costs | |
| Startup costs | 4% FCI |
| Working capital | 15% FCI |
| Costs of licensing, research and development | 7.5% FCI |
| Allowance funds used during construction | 7.5% FCI |

**Table 6: Cost correlations for cascaded ORC's components.**

| Equipment | Cost Correlation | Equation Number | References |
|---|---|---|---|
| Pump | $PEP_p = 378\left[1+\left(\frac{1-0.808}{1-\eta_p}\right)\right]W_p^{0.71}$ | 13 | [34] |
| Generator | $PEP_{gen} = 60W_{gen}^{0.95}$ | 14 | [7] |
| Turbine | $PEP_T = -16610 + 716W_T^{0.80}$ | 15 | [35] |
| Evaporator | $PEC_{eva} = 3650\left(\frac{\dot{q}_{eva}}{\Delta T_{lm,eva}}\right)^{0.8}$ | 16 | [7] |
| Condenser | $PEP_C = 30800 + 890A_C^{0.81}$ | 17 | [36] |
| Recuperator | $PEC_{rec} = 11256 + 579A^{0.8}$ | 18 | [34] |

The levelized cost of electricity (*LCOE*) is expressed in Eqn. (19) [37]. As stated in Eqn. (20) [4], the total production cost is the total of fixed costs and total annual direct cost of manufacturing ($C_{DMC}$). Table **7** displays the computation of $C_{DMC}$ and $C_{FIX}$.

$$LCOE = \frac{C_{TIC} + \sum_{t=1}^{21} \frac{C_{TPC}}{(1+i)^t}}{\sum_{t=1}^{21} \frac{M_{el}}{(1+i)^t}} \tag{19}$$

with

$$C_{TPC} = C_{DMC} + C_{FIX} \tag{20}$$

and

$$M_{el} = H_{annual} \times W_{net}^{elec} = 0.9 \times 365 \times 24 \times W_{net}^{elec} \tag{21}$$

where *LCOE* is the levelized cost of electricity (US$/kWh), $M_{el}$ is the annual generated electrical energy (kWh), *i* is the annual discount rate, set 7% [38], *t* is the operational year (*t*=1,2,3,4....). $C_{TPC}$ and fixed cost, as given in Eqn. (20) [4]. The computation of $C_{DMC}$ and $C_{FIX}$ are shown in Table **7**.

**Table 7: Computation of direct manufacturing and fixed costs [4, 39-44].**

| Particular | Description | Formula |
|---|---|---|
| Direct cost | Direct manufacturing cost | $C_{DMC}$ |
| Utilities | Cooling water | 14.8 US$/1000m$^3$ |
| Maintenance | Wages and benefits | $C_{WB}$ = 3.5% $C_{TDC}$ |
| | Salaries and benefits | $C_{SB}$ = 25% *CWB* |
| | Materials and services | $C_{MS}$ = $C_{WB}$ |
| | Maintenance overhead | $C_{MO}$ = 5%$C_{WB}$ |
| Fixed costs | Fixed manufacturing costs | $C_{FIX}$ |
| Property taxes and insurance | Cost of property taxes and liability insurance | $C_{PI}$ = 2% $C_{TDC}$ |

# 4. Environmental Performance

It is assumed that the mainly energy consumption of the industrial gas turbine model SGT 400 is natural gas. Moreover, the environmental performance focuses on the carbon dioxide ($CO_2$) emission offset by utilizing the waste heat from the industrial gas turbine. The $CO_2$ offset by using the electricity output from the ORC system can be calculated by using Eqn. (22) [7, 45-50]:

$$E_{CO2} = P_{net} \times h \times \beta_{CO2} \tag{22}$$

where $E_{CO2}$, $P_{net}$, *h*, and $\beta_{CO2}$ stand for the $CO_2$ reduced by generating the electricity from the waste heat ($tCO_2eq$), net power output of the cascaded ORC (kW), annual operating hours of the ORC system (8700 h/year), and $CO_2$ emission factor, which represents the emission to the atmosphere per unit of electricity produced (kg CO2-eq/kWh).

# 5. Validation

The numerical model of this study is validated by the data from the literature with cascaded ORCs operated under the same heat source and heat sink. The data from Rashwan *et al*. [32] employed a cascaded ORC operated at the heat source of 450 °C, mass flow rate of 40 kg/s and propane as a working fluid. For comparison, the numerical model (cascade ORC) in this study was run with a similar heat source, mass flow rate, and working fluid as in the literature. Table **8** shows further operating parameters for model validation. As demonstrated in Table **3**, the numerical results are tremendously consistent with the literature. The net power output and thermal efficiency are somewhat higher than published values, resulting in a small percentage inaccuracy. This is because the numerical model fails to account for the working fluid's pressure drop in the heat exchanger and tube.

# 6. Results and Discussion

## 6.1. Thermodynamic Performance

The effect of expander inlet temperature on the net power output ($P_{net}$) of a single (black curve) and dual (blue curve) fluid cascaded ORCs is illustrated in Fig. (**2a**-**d**). In this analysis, the expander inlet temperature is varied

from 500 to 723 K, while the expander inlet pressure and condensation temperature remain constant at 5500 kPa and 303 K. The primary *y*-axis of Fig. (**2**) shows the $P_{net}$ generated by the single and dual fluid cascaded ORCs while the secondary *y*-axis shows the percentage increase in net power output ($\%\Delta P_{net}$) from the single to dual fluid cascaded ORC. Fig. (**2a**-**d**) show the performance of different working fluids on the $P_{net}$ generated while varying expander inlet temperature. It can be seen from Fig. (**2a**-**d**) that when the expander inlet temperature increases, the $P_{net}$ increases in all working fluids and cascaded ORCS. But in all working fluids, the dual fluid cascaded ORC showed a greater $P_{net}$ than the single fluid cascaded ORC. As per Fig. (**2a**-**d**), toluene+R601a, benzene+R601a, acetone+R601a, and cyclopentane+R601a yielded approximately 791.55, 832.06, 1225.94, and 1245.11 kW, respectively. It is discovered that for all working fluids, the highest $P_{net}$ is obtained at the highest expander inlet temperature. Cyclopentane+R601a showed the greatest $P_{net}$ among all fluid choices. On the contrary, the $P_{net}$ in the single fluid cascaded ORC seemed to increase with expander inlet temperature. Likewise, the highest $P_{net}$ of the single fluid cascaded ORC is attained when the expander inlet temperature is 723 K. In all the fluids, the $P_{net}$ of the single fluid cascaded ORC is not greater than that of the dual fluid cascaded ORC. However, $P_{net}$ increases similarly for both single and dual fluid cascaded ORCs. Furthermore, toluene, benzene, acetone, and cyclopentane yielded approximately 700.56, 723.01, 1091.90, and 1170.27 kW, respectively. The cyclopentane exhibited a good performance on $P_{net}$ and reached a maximum of 1170.27 kW at 723 K. When comparing all fluids in all ORCs, cyclopentane performed well due to its low boiling point, which allows it to evaporate easily at low temperatures. However, cyclopentane is extremely flammable, thus extra measures must be taken [24].

**Table 8: Comparison of present results with Ref. [32].**

| Parameter | Single Fluid Cascade ORC | | |
|---|---|---|---|
| | Ref. [22] | This Study | %Error |
| Heat source temperature, °C | 460 | 430 | 6.5 |
| Expander inlet temperature, °C | 200 | 210 | -5.0 |
| Condensation temperature, °C | 40 | 40 | - |
| Peak net power output, kW | 1920.967 | 1949.987 | -1.5 |
| Thermal efficiency, % | 19.227 | 19.352 | -0.7 |

The second *y*-axis of Fig. (**2a**-**d**) shows the percentage increase in $P_{net}$ ($\%\Delta P_{net}$) (red curve) from the single to dual fluid cascaded ORC. It can be seen that in all working fluids, $\%\Delta P_{net}$ is high when the expander inlet temperature is low and keeps decreases when the expander inlet temperature increases. As observed from second *y*-axis of Fig. (**2a**-**d**), the highest $\%\Delta P_{net}$ indicates the large difference in $P_{net}$ from the single to dual fluid cascaded ORC when operates at low expander inlet temperature. From Fig. (**2a**-**d**), the highest $\%\Delta P_{net}$ is observed to reach 30, 33, 43, and 24 %, respectively. It can be seen that operating acetone and acetone+R601a in the single and dual fluid cascaded ORCs, respectively, can result in a significant change in $P_{net}$. Conversely, cyclopentane and cyclopentane+R601a in the single and dual fluid cascaded ORCs, respectively, resulted in lowest $\%\Delta P_{net}$ when operated in the low expander inlet temperature. This can be attributed by the molecular weight of the cyclopentane. At the highest expander inlet temperature, the observed $\%\Delta P_{net}$ as shown in Fig. (**2a**-**d**) were 11, 13, 11, and 6 %, respectively. The main finding is that at high expander inlet temperatures, there is no substantial change in $P_{net}$, especially for cyclopentane.

On the side, the effect of condensation temperature on the $P_{net}$ of a single (black curve) and dual (blue curve) fluid cascaded ORCs is illustrated in Fig. (**2e**-**h**). The condensation temperature is varied from 293 to 323 K while keeping constant expander inlet temperature at 500 K. For both single and dual fluid cascaded ORCs $P_{net}$ is seemed to slightly increase with the condensation temperature. As seen in the primary *y*-axis of Fig. (**2e**-**h**), the highest $P_{net}$ of the toluene+R601a, benzene+R601a, acetone+R601a, and cyclopentane+R601a reached approximately 217.61, 356.16, 345.59, and 338.09 kW, respectively. Despite the sluggish increase, all of the $P_{net}$ were achieved at the maximum condensation temperature. When compared with the single fluid cascaded ORC, the highest $P_{net}$ of the toluene, benzene, acetone, and cyclopentane reached approximately 160.59, 248.75, 211.70, and 263.32 kW, respectively. Similarly, the highest $P_{net}$ values were observed at the maximum condensation

temperature. This result aligned with the previous work [35] As seen in the secondary *y*-axis of Fig. (**2e**-**h**), there is a large increase in $P_{net}$ (red curve) ($\%\Delta P_{net}$) from single to dual fluid cascaded ORC when operating at low condensation temperature. In all working fluids, $\%\Delta P_{net}$ is high when the condensation temperature is low and keeps decreases when the condensation temperature increases. From Fig. (**2e**-**h**), the highest $\%\Delta P_{net}$ is observed to

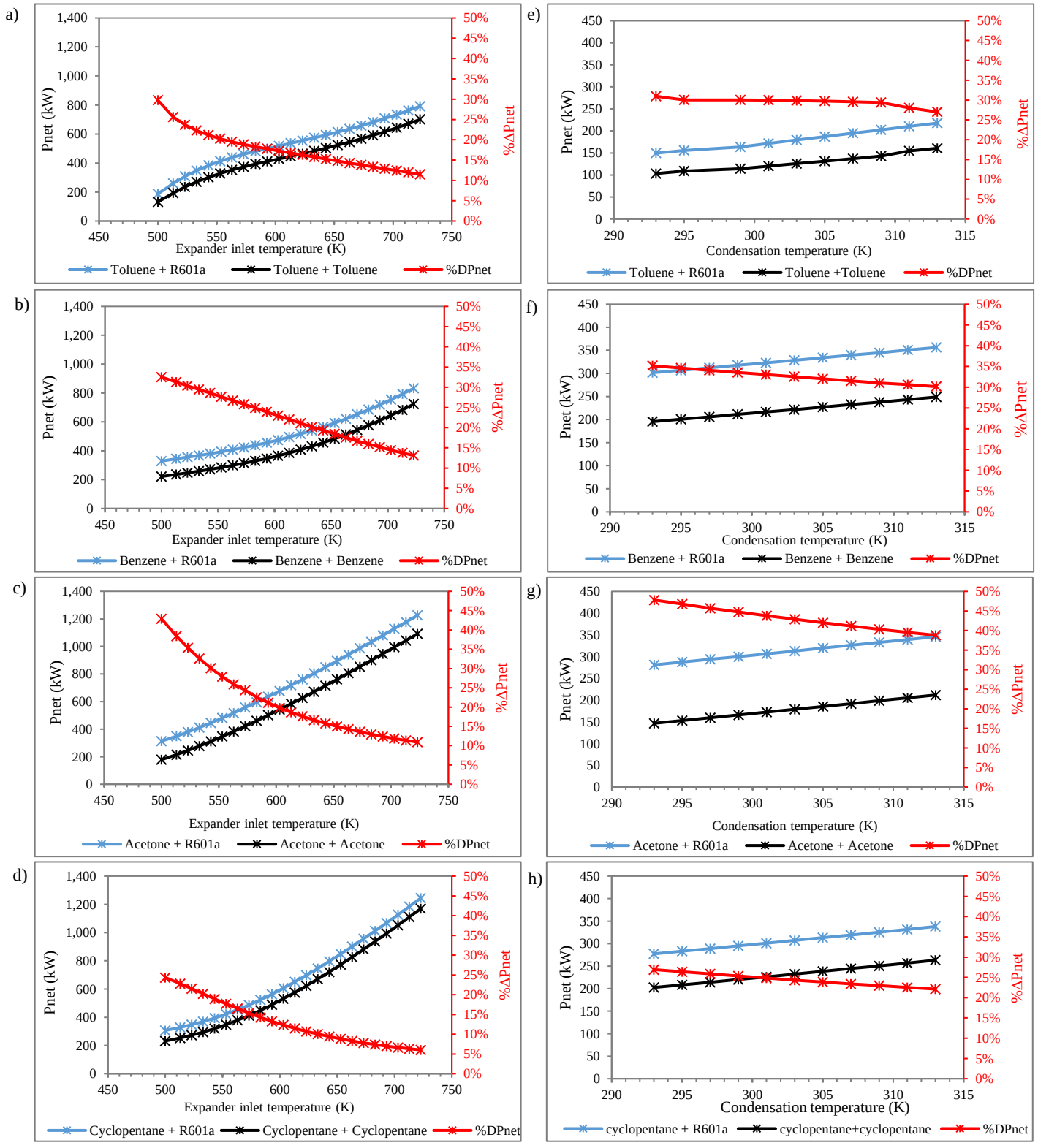


**Figure 2:** The variation of $P_{net}$ in a single and dual fluid ORCs under the conditions of (**a-d**) expander inlet temperature and (**e-h**) condensation temperature.

reach 31, 35, 48, and 27 %, respectively. Similar to the condition of expander inlet temperature, it is discovered that operating acetone and acetone+R601a in the single and dual fluid cascaded ORCs, respectively, can result in a considerable increase in $P_{net}$. The effect of the expander inlet temperature on thermal efficiency ($\eta_{th}$) of single and dual fluid cascaded ORCs is shown in Fig. (**3a**-**d**). The $\eta_{th}$ as illustrated in Fig. (**3a**-**d**). tends to increase with the expander inlet temperature. As illustrated in the primary *y*-axis of Fig. (**3a**-**d**), the $\eta_{th}$ of the single fluid cascaded ORC varied from 7.42 to 22.21; 11.72 to 23.19; 8.35 to 30.79; and 11.57 to 33.25 % when operates with toluene, benzene, acetone, and cyclopentane, respectively. The single fluid cascaded ORC attained the highest $\eta_{th}$ of 33.25 % while operating with cyclopentane at 723 K. On the contrary, $\eta_{th}$ of the dual fluid cascaded ORC varied from 10.28 to 25.05; 17.12 to 26.90; 15.75 to 37.23; and 15.10 to 35.57 % when operates with toluene+R601a, benzene+R601a, acetone+R601a, and cyclopentane+R601a, respectively. The dual fluid cascaded ORC reached the highest $\eta_{th}$ of 37.23 % while operating with acetone+R601a at 723 K.

Comparing the trend of $\eta_{th}$ ($\%\Delta\eta_{th}$) in the secondary y-axis of Fig. (**3a-d**), the downtrend is similar to that of $\%\Delta P_{net}$. The $\%\Delta\eta_{th}$ is low at low expander inlet temperature and increases with increase in expander inlet temperature. This illustrates the considerable increase in $\eta_{th}$ at high expander inlet temperatures when shifting from single to dual cascaded ORC. The peak $\%\Delta\eta_{th}$ (47%) is observed when acetone is used as a working fluid at 500 K expander inlet temperature. The effect of condensation temperature on $\eta_{th}$ of single and dual fluid cascaded ORCs is shown in Fig. (**3e-h**). It can be observed that in Fig. (**3e-h**), $\eta_{th}$ slightly increases with the condensation temperature. As illustrated in the primary *y*-axis of Fig. (**3e-h**), the $\eta_{th}$ of the single fluid cascaded ORC varied from 6.02 to 8.92; 10.36 to 13.15; 6.98 to 9.78; and 10.10 to 13.14 % when operates with toluene, benzene, acetone, and cyclopentane, respectively. On the contrary, $\eta_{th}$ of the dual fluid cascaded ORC varied from 8.29 to 11.84; 15.64 to 18.69; 14.04 to 17.54; and 13.57 to 16.74 % when operates with toluene+R601a, benzene+R601a, acetone+R601a, and cyclopentane+R601a, respectively. The peak $\eta_{th}$ reached 18.69 % when dual fluid cascaded ORC is run on benzene+R601a at 723 K. Overall, increasing the expander inlet temperature yielded to the highest $P_{net}$ and $\eta_{th}$ of 1245 kW and 37.23%, respectively, with acetone+R601a as a working fluid. This resulted in an increase of $\%\Delta P_{net}$ and $\%\Delta\eta_{th}$ of around 43 and 47 %, respectively.

### 6.2. Economic Performance

The variation of net present value (NPV) with expander inlet temperature for the single and dual fluid cascade ORCs can be seen in Fig. (**4a-d**). It can be seen that both single and dual fluid cascaded ORCs have negative NPVs at low expander inlet temperatures, grow slightly toward zero NPV, then after rise quickly with expander inlet temperature. From Fig. (**4a-d**), the dual fluid cascaded ORC has the positive NPV at expander inlet temperature of 603, 623, 553, and 583 K when run under toluene+R601a, benzene+R601a, acetone+R601a, and cyclopentane+ R601a, respectively. Furthermore, the highest NPV reached US$ 90,128.55, 103,45.02, 234,485.59, and 240,853.55, respectively, and were observed at 723 K. It can be deduced that acetone+R601a and cyclopentane+R601a have a wide range of positive NPVs compared to toluene+R601a and benzene+R601a. When operated under toluene, benzene, acetone, and cyclopentane, respectively, NPV of the single fluid cascaded ORC turns positive at expander inlet temperatures of 653, 673, 603, and 603 K. Overall, this implies that the single and dual fluid cascade ORCs must operate above 600 and 550 K, respectively, at the expander inlet temperatures for the plants to be economically feasible.

Fig. (**4e-h**) depict the variation of NPV with condensation temperature for the single and dual fluid cascade ORCs. Fig. (**4e-h**) show that both single and dual fluid cascaded ORCs exhibit a negative NPV at all condensation temperatures. This could be related to the low power generated under this condition.

Fig. (**5a-d**) depict the variation of levelized cost of electricity (LCOE) with expander inlet temperature for the single and dual fluid cascade ORCs. As illustrated in Fig. (**5a-d**), both single and dual fluid cascaded ORCs have the highest LCOEs at the low expander inlet temperatures, which decrease exponentially as expander inlet temperatures rise. Furthermore, the lowest LCOEs occur at the highest expander inlet temperatures (723 K). This can be attributed by the highest $P_{net}$ generation that occurs at the highest expander inlet temperatures. From Fig. (**5a-d**), the dual fluid cascaded ORC showed the lowest LCOE of 0.0403, 0.0263, 0.0172, and 0.0177 US$/kWh when run under toluene+R601a, benzene+R601a, acetone+R601a, and cyclopentane+R601a, respectively. Furthermore, the lowest LCOE of 0.0172 US$/kWh was observed when run with acetone+R601a. On the contrary, single fluid

cascaded ORC attained the lowest LCOE of 0.0480, 0.0335, 0.0223, and 0.0179 US$/kWh when run under toluene, benzene, acetone, and cyclopentane, respectively. For this case, the lowest LCOE of 0.0179 US$/kWh is observed when run with cyclopentane. The lowest LCOE of the dual fluid cascaded ORC is 1.1% lower than that of the single fluid cascaded ORC. The lower LCOE of the dual fluid cascaded ORC shows a promising energy selling price, which

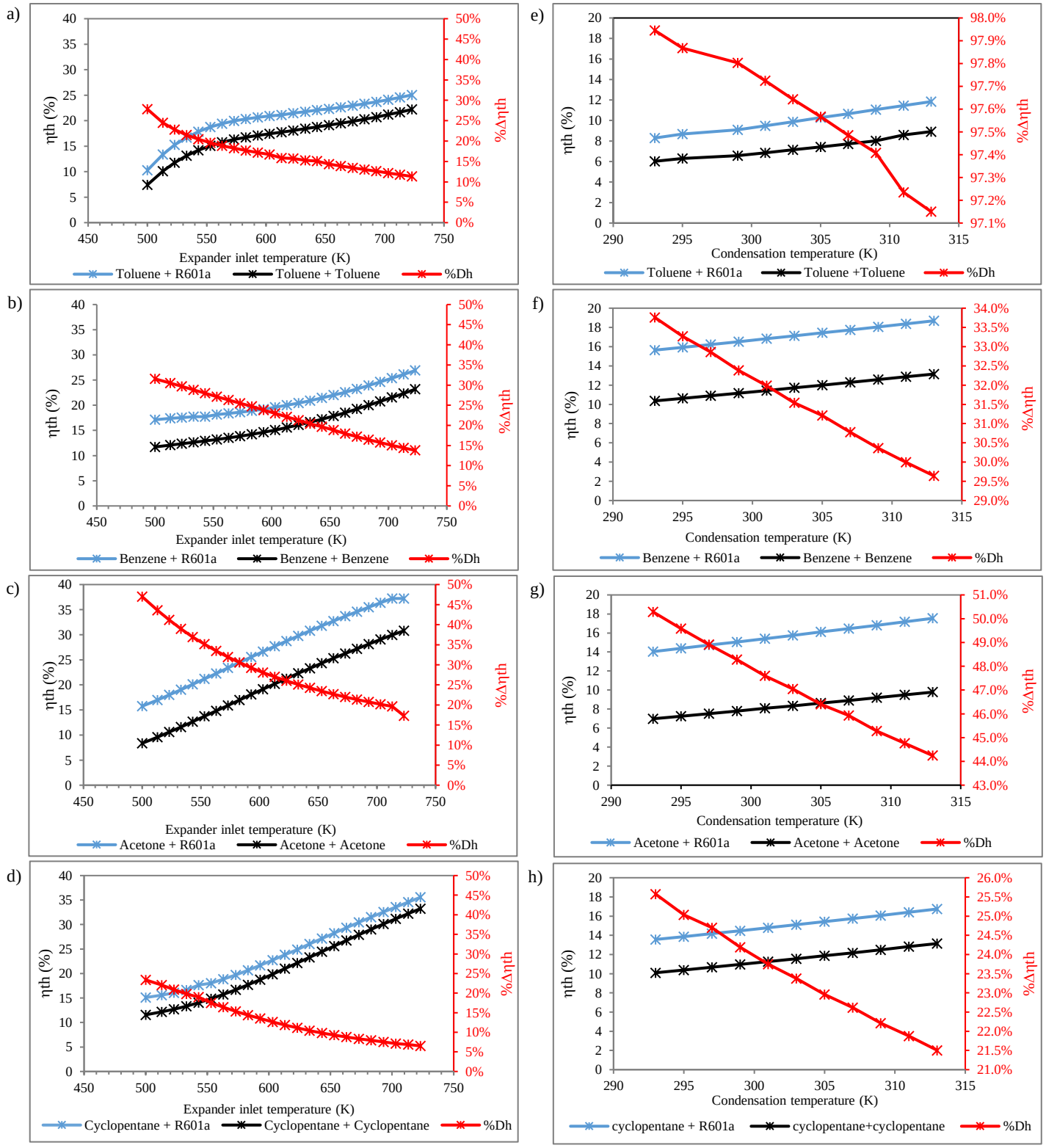


**Figure 3:** The variation of $\eta_{th}$ of a single and dual fluid ORCs under the conditions of (**a-d**) expander inlet temperature and (**e-h**) condensation temperature.

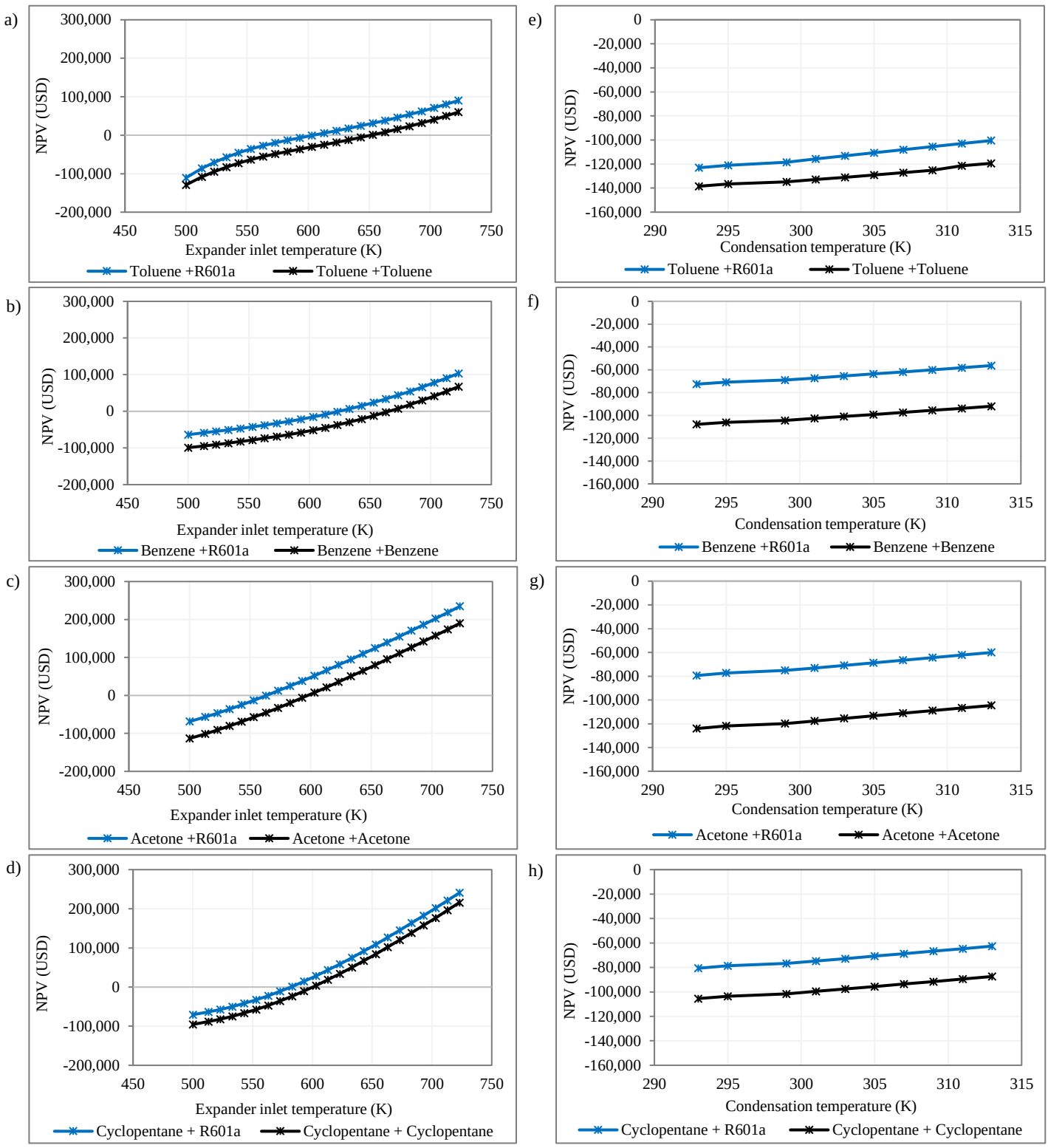


**Figure 4:** The variation of NPV of a single and dual fluid ORCs under the conditions of (**a-d**) expander inlet temperature and (**e-h**) condensation temperature.

encourages project execution. Fig. (**5e-h**) illustrate the variation of levelized cost of electricity (LCOE) with condensation temperature for the single and dual fluid cascade ORCs. As for the case of expander inlet temperature, both single and dual fluid cascaded ORCs have the highest LCOEs at the low condensation temperatures, which decrease as condensation temperatures rise. It is also indicated that the lowest LCOEs occur

at the highest expander inlet temperatures (723 K). As shown in Fig. (**5e-h**), the dual fluid cascaded ORC showed the lowest LCOE of 0.1090, 0.0630, 0.0700, and 0.0730 US$/kWh when run under toluene+R601a, benzene+R601a, acetone+R601a, and cyclopentane+R601a, respectively. The lowest LCOE of 0.0630 US$/kWh is achieved when run using benzene+R601a. In contrast, single fluid cascaded ORC attained the lowest LCOE of 0.1490, 0.0950, 0.1180,

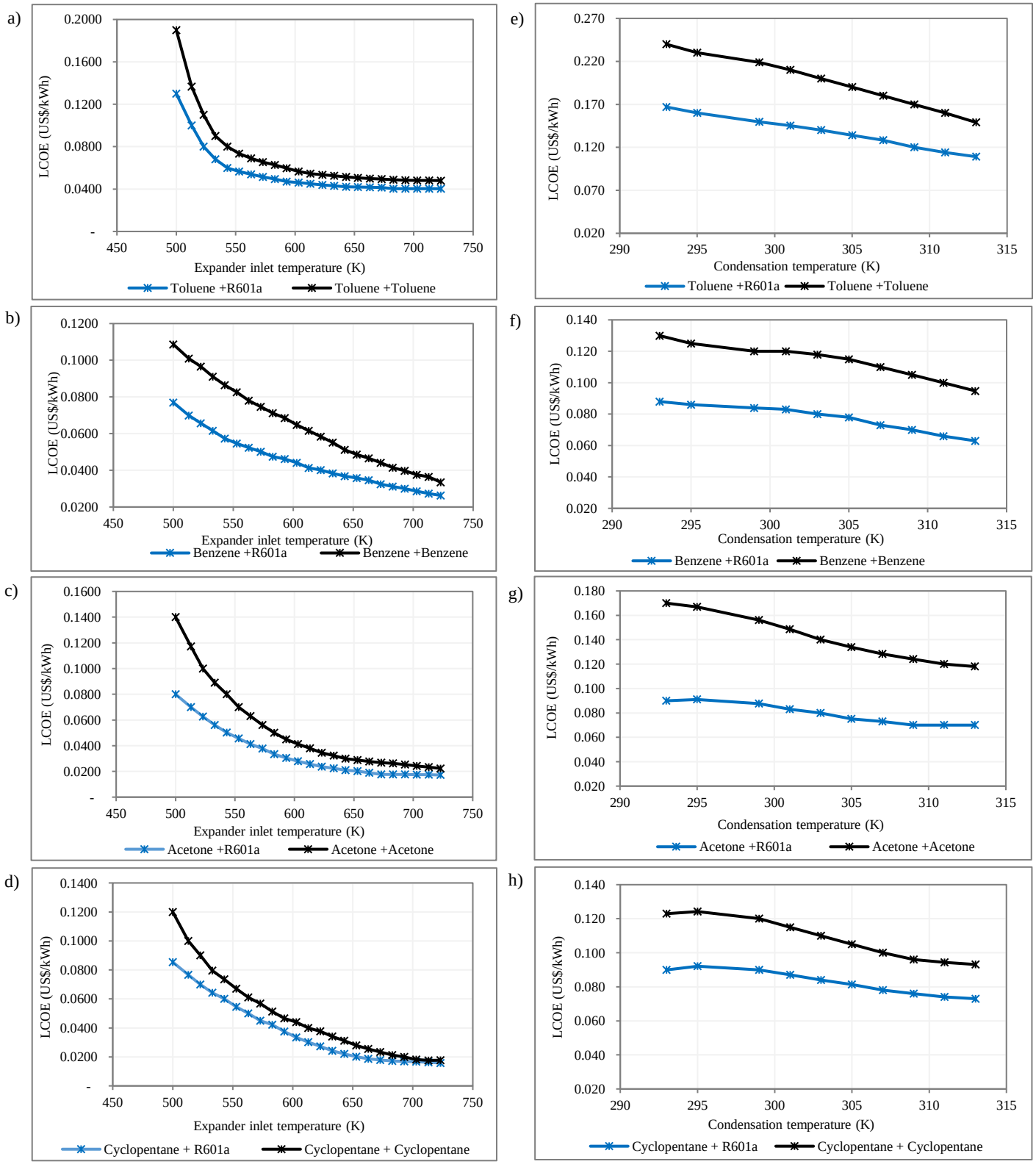


**Figure 5:** The variation of LCOE of a single and dual fluid ORCs under the conditions of (**a-d**) expander inlet temperature and (**e-h**) condensation temperature.

and 0.0930 US$/kWh for toluene, benzene, acetone, and cyclopentane, respectively. When comparing the lowest LCOEs, dual fluid cascaded ORC is 32.3% cheaper than its counterpart. In the case of dual fluid cascaded ORC, comparison of the lowest LCOE in variation of expander inlet temperatures and condensation temperatures reveals that varying expander inlet temperatures drop the energy price by 22.15 and 63.03%; 12.50 and 58.25; 11.11 and 68.14%; 5.11 and 75.75% for toluene+R601a, benzene+R601a, acetone+R601a, and cyclopentane+R601a, respectively. Because of the large drop in energy prices, varying the expander inlet temperature becomes a more

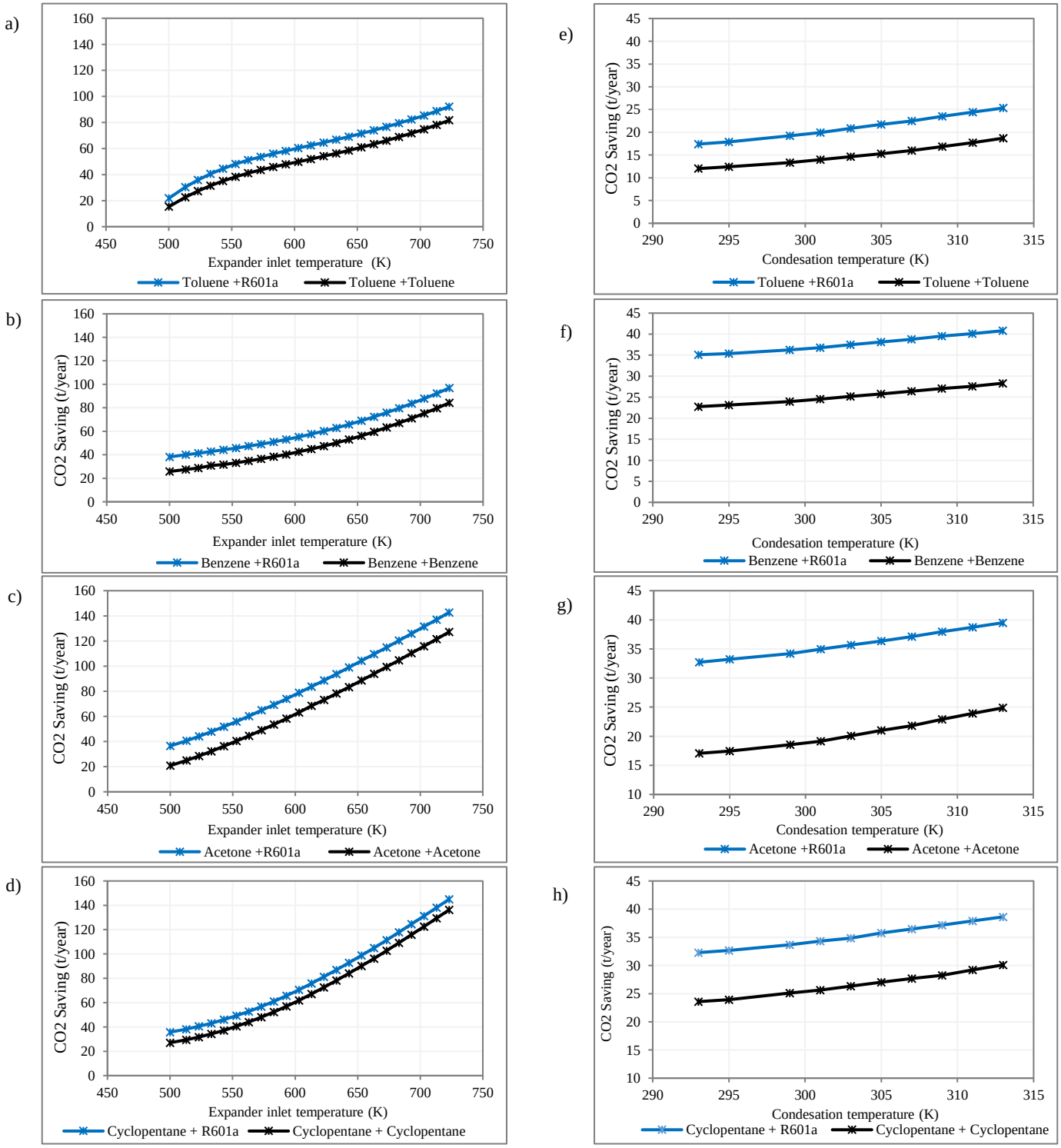


**Figure 6:** The variation of $CO_2$ saving of a single and dual fluid ORCs under the conditions of (**a-d**) expander inlet temperature and (**e-h**) condensation temperature.

beneficial condition for operating the dual fluid cascaded ORC. On the other hand, electricity cost in Thailand approaches 0.122 US$/kWh, therefore the reached LCOEs of single and dual fluid ORCs could have promise for infiltrating the Thai electricity market, especially for the dual fluid cascaded ORC.

### 6.3. Environmental Performance

Fig. (**6a-d**) depict the variation of carbon dioxide saving ($CO_2$ saving) with expander inlet temperature for the single and dual fluid cascade ORCs. From Fig. (**6a-d**), it can be seen that both single and dual fluid cascaded ORCs have the lowest $CO_2$ savings per year at the low expander inlet temperatures, and increase exponentially as expander inlet temperatures rise. Furthermore, the highest $CO_2$ savings per year occur at the highest expander inlet temperatures (723 K). The dual fluid cascaded ORC achieved the environmental saving by reducing approximately 92.15, 96.87, 142.73, and 144.96 $tCO_{2\text{-eq}}$/year when run under toluene+R601a, benzene+R601a, acetone+R601a, and cyclopentane+R601a, respectively. It is observed that the maximum $CO_2$ saving is achieved by cyclopentane+R601a at expander inlet temperature 723 K. In the single fluid cascaded ORC, achieved the environmental saving by reducing about 81.63, 84.18, 127.12, and 136.25 $tCO_{2\text{-eq}}$/year when run under toluene, benzene, acetone, and cyclopentane, respectively. When it comes to maximal $CO_2$ reduction, it is clear that dual fluid cascaded ORCs may save the environment by approximately 6.39% more than single fluid cascaded ORC.

Fig. (**6e-h**) show the variation of carbon dioxide saving ($CO_2$ saving) with condensation temperature for the single and dual fluid cascade ORCs. It can be seen that there is a slight increase in environment saving as condensation temperature increases. As seen in Fig. (**6e-h**), dual fluid cascaded ORC achieved the environmental saving by reducing approximately 25.33, 40.81, 39.50, and 38.63 $tCO_{2\text{-eq}}$/year when run under toluene+R601a, benzene+R601a, acetone+R601a, and cyclopentane+R601a, respectively. The single fluid cascaded ORC produced environmental saving by reducing about 18.70, 28.32, 24.88, and 30.10 $tCO_2$/year when run under toluene, benzene, acetone, and cyclopentane, respectively. These $CO_2$ savings are related with the emission of the fuel that would provide the same amount of energy as generated by these ORCs. By considering the natural gas engine's conversion factors of 65 g(fuel)/kWh [23] and 0.0133 $kgCO_2$/kWh, as well as the peak $P_{net}$ of 1245.11 kW (Fig. **2d**), a fuel reduction of approximately 708.9 t/year is projected.

## 7. Conclusions

In this study the potential of cascade ORC operated under single and dual working fluid is investigated. The comprehensive thermodynamic analysis including the variation of expender inlet temperature and condensation temperature is analyzed, economic benefit focuses on NPV and LCOE and Environmental side, amount of $CO_2$ saving is evaluated. The key finding is summarized as follows.

- The single and dual fluid cascaded ORCs achieved the highest $P_{net}$ of 1170.27 and 1245.11 kW, respectively at an expander inlet temperature of 723 K. The dual fluid cascaded ORC showed the significant increase in $P_{net}$ ($\%\Delta P_{net}$) for about 43% at the lowest expander inlet temperature (500 K) and small $\%\Delta P_{net}$ at the highest expander inlet temperature. Variations in condensation temperature resulted in peak $P_{net}$ values of 263.32 and 356.16 kW in the single and dual fluid cascaded ORCs, respectively, which are greatly exceeded by the condition of expander inlet temperature.
- In terms of thermal efficiency ($\eta_{th}$), single and dual fluid cascaded ORCs reached 33.25 and 37.23 %, respectively at an expander inlet temperature of 723 K. The dual fluid cascaded ORC showed the significant increase in $\eta_{th}$ ($\%\Delta\eta_{th}$) at the lowest expander inlet temperature of 500 K.
- Acetone and acetone+R601a in the single and dual fluid cascaded ORCs resulted in the generation of peak $P_{net}$ at the highest expander inlet temperature, but cyclopentane and benzene+R601a produced peak $P_{net}$ at the highest condensation temperature.
- On the economic side, the NPV for a single fluid cascade ORC turned positive at expander inlet temperature of 653 K; however, acetone and cyclopentane turned positive sooner than other fluids because of their higher molecular weight and their resulted improved $P_{net}$. In contrast, NPV for a dual fluid turned positive at expander inlet temperature of 553 K with cyclopentane +R601a and acetone +601a, and produced a wide range of NPV when expander inlet temperature varied.

- When the expander inlet temperatures were varied, single and dual fluid cascaded ORCs with cyclopentane and cyclopentane+R601a had the lowest LCOEs of 0.0177 and 0.0158 US$/kWh, respectively, which are lower than Thai electricity price. The lowest LCOE of the dual fluid cascaded ORC is 1.1% lower than that of the single fluid cascaded ORC. In that case, the lower LCOEs of dual fluid ORC could have promise for infiltrating the Thai electricity market.
- In environmental saving, single and dual fluid cascaded ORCs reducing carbon dioxide ($CO_2$) emissions for about 136.25 and 144.96 $tCO_{2\text{-eq}}$/year when run under cyclopentane and cyclopentane+R601a, respectively. When it comes to maximum $CO_2$ reduction, dual fluid cascaded ORCs outperform single fluid cascaded ORCs by roughly 6.39%.

Overall, dual fluid cascaded ORC outperformed single fluid cascaded ORC in all thermodynamic, economic and environmental metrics. Variations in expander inlet temperatures have a greater impact on the performance of dual fluid cascaded ORC than variations in condensation temperatures. Different working fluids, particularly cyclopentane, performed exceptionally well under these conditions. However, safety considerations must be considered when operating at high temperatures that exceed their limitations.

# Nomenclature

| | | |
|---|---|---|
| C | = | Condenser |
| $E_{CO2}$ | = | $CO_2$ reduced by generating electricity from waste heat ($tCO_2e$) |
| EXP | = | Expander |
| HEX | = | Heat exchanger |
| $I$ | = | Income (US$) |
| $m$ | = | Mass flow rate of working fluid (kg/s) |
| ORC | = | Organic Rankine cycle |
| P | = | Pump |
| $P_{net}$ | = | Net power output (kW) |
| $Q$ | = | Heat gain or rejected (kW) |
| T | = | Temperature (K) |
| $TIC$ | = | Total investment cost (US$) |
| $W$ | = | Work net (kW) |
| $\beta_{CO2}$ | = | $CO_2$ emission factor (tCO2e/kg) |

**Subscript**

| | | |
|---|---|---|
| cond | = | Condenser |
| cw | = | Cooling water |
| exp | = | Expander |
| ext,g | = | Exhaust gas |
| ext,in | = | Exhaust in |
| g | = | Generator |
| in | = | Inlet of each point |
| net | = | Net |
| out | = | Outlet of each point |
| p | = | Pump |
| t | = | Turbine |
| th | = | Thermal |
| wf | = | Working fluid |

**Greek Symbol**

$\eta$ = Efficiency

$\eta_{th}$ = Thermal efficiency

## Conflict of Interest

The authors declare that they have no known competing financial interests or personal relationships that could have appeared to influence the work reported in this paper.

## Funding

This research was financially supported by the Malaysia-Thailand Joint Authority (MTJA) and Universiti Teknologi Malaysia (UTM).

## Authors' Contribution

Gerutu Bosinge Gerutu: Conceptualization, Formal analysis, Writing –original draft, Investigation, Methodology, Data curation. Yossapong Laoonual: Writing –review, and Funding acquisition,

## Acknowledgments

The authors would like to express their gratitude to The Joint Graduate School of Energy and Environment, King Mongkut's University of Technology Thonburi, and the Center for Energy Technology and Environment, Ministry of Higher Education, Science, Research, and Innovation-Thailand for their support.

## References

[1] White MT, Read MG, Sayma AI. Making the case for cascaded organic Rankine cycles for waste-heat recovery. Energy. 2020; 211: 118912. https://doi.org/10.1016/j.energy.2020. 118912

[2] IEA. Global Energy Review 2020. IEA; Paris: April 2020. Available from: https://www.iea.org/reports/global-energy-review-2020 (Accessed on January 2024).

[3] Hu K, Zhang Y, Yang W, Liu Z, Sun H, Sun Z. Energy, exergy, and economic (3E) analysis of transcritical carbon dioxide refrigeration system based on ORC system. Energies. 2023; 16(4): 1675. https://doi.org/10.3390/en16041675

[4] Singh DV, Pedersen E. A review of waste heat recovery technologies for maritime applications. Energy Convers Manag. 2016; 111: 315-28. https://doi.org/10.1016/j.enconman.2015.12. 073

[5] Lu P, Liang Z, Luo X, Xia Y, Wang J, Chen K, *et al*. Design and optimization of organic rankine cycle based on heat transfer enhancement and novel heat exchanger: a review. Energies. 2023; 16(3): 1380. https://doi.org/10.3390/en16031380

[6] Watson SM. Greenhouse gas emissions from offshore oil and gas activities—relevance of the paris agreement, law of the sea, and regional seas programmes. Ocean Coast Manag. 2020; 185: 104942. https://doi.org/10.1016/j.ocecoaman.2019.104942

[7] Ma Q, Chen Y, Liu A, Jiang Q. Benefit analysis of organic Rankine cycle power generation by using waste heat recovery in Refinery. E3S Web Conf. 2022; 352: 02014. https://doi.org/10.1051/e3sconf/202235202014

[8] Chen T, Zhuge W, Zhang Y, Zhang L. A novel cascade organic Rankine cycle (ORC) system for waste heat recovery of truck diesel engines. Renew Sustain Energy Rev. 2017; 138: 210-23. https://doi.org/10.1016/j.enconman.2017.01.056

[9] Jouhara H, Khordehgah N, Almahmoud S, Delpech B, Chauhan A, Tassou SA. Waste heat recovery technologies and applications. Therm Sci Eng Prog. 2018; 6: 268-89. https://doi.org/10.1016/j.tsep.2018.04.017

[10] Mahmoudi A, Fazli M, Morad MR. A recent review of waste heat recovery by Organic Rankine Cycle. Appl Therm Eng. 2018; 143: 660-75. https://doi.org/10.1016/j.applthermaleng.2018.07.136

[11] Nandhini R, Sivaprakash B, Rajamohan N. Waste heat recovery at low temperature from heat pumps, power cycles and integrated systems–Review on system performance and environmental perspectives. Sustain Energy Technol Assessments. 2022; 52: 102214. https://doi.org/10.1016/j.seta.2022.102214

[12] Raab F, Böse L, Klein H, Opferkuch F. Steam storage rankine cycle for unutilized applications in distributed high-temperature waste heat recovery. Energies. 2024; 17(4): 920. https://doi.org/10.3390/en17040920

[13] Blanquart F. Perspectives for power generation from industrial waste heat recovery (Thesis). KTH School of Industrial Engineering and Management Energy Technology; Stockholm: 2017.

[14] Forman C, Muritala IK, Pardemann R, Meyer B. Estimating the global waste heat potential. Renew Sustain Energy Rev. 2016; 57: 1568-79. https://doi.org/10.1016/j.rser.2015.12.192

[15] Lebedevas S, Čepaitis T. Complex use of the main marine diesel engine high- and low-temperature waste heat in the organic rankine cycle. J Mar Sci Eng. 2024; 12: 521. https://doi.org/10.3390/jmse12030521

[16] Konur O, Yuksel O, Korkmaz SA, Colpan CO, Saatcioglu OY, Muslu I. Thermal design and analysis of an organic rankine cycle system utilizing the main engine and cargo oil pump turbine-based waste heats in a large tanker ship. J Clean Prod. 2022; 368: 133230. https://doi.org/10.1016/j.jclepro.2022.133230

[17] Larsen U, Pierobon L, Haglind F, Gabrielii C. Design and optimisation of organic Rankine cycles for waste heat recovery in marine applications using the principles of natural selection. Energy. 2013; 55: 803-12. https://doi.org/10.1016/j.energy.2013.03.021

[18] Lion S, Michos CN, Vlaskos I, Taccani R. A thermodynamic feasibility study of an Organic Rankine Cycle (ORC) for heavy-duty diesel engine waste heat recovery in off-highway applications. Int J Energy Environ Eng. 2017; 8: 81-98. https://doi.org/10.1007/s40095-017-0234-8

[19] Ritchie H, Roser M, Rosado P. $CO_2$; and greenhouse gas emissions. Our world in data, January 2023. Available from: https://ourworldindata.org/co2-and-greenhouse-gas-emissions (Accessed on January 2024).

[20] Tian H, He Z, Zhang X, Li L, Cai J, Wang X, *et al*. Comparison study of four typical orc configurations for different waste heat characteristics of engine. Int J Energy Res. 2023; 8865282. https://doi.org/10.1155 /2023/8865282

[21] Javanshir A, Sarunac N. Thermodynamic analysis of a simple Organic Rankine Cycle. Energy. 2017; 118: 85-96. https://doi.org/10.1016/j.energy.2016.12.019

[22] Valencia, OG, Cárdenas GJ, Duarte FJ. Exergy, economic, and life-cycle assessment of ORC system for waste heat recovery in a natural gas internal combustion engine. Resources. 2020; 9(1): 2. https://doi.org/10.3390/resources9010002

[23] Reis LMM, Gallo RLW. Study of waste heat recovery potential and optimization of the power production by an Organic Rankine Cycle in an FPSO unit. Energy Convers Manag. 2018; 157: 409-22. https://doi.org/10.1016/j.enconman.2017.12.015

[24] Zare V. A comparative exergoeconomic analysis of different ORC configurations for binary geothermal power plants. Energy Convers Manag. 2015; 105: 127-38. https://doi.org/10 .1016/j.enconman.2015.07.073

[25] Ren J, Cao Y, Long Y, Qiang X, Dai Y. Thermodynamic comparison of gas turbine and ORC combined cycle with pure and mixture working fluids. J Energy Eng. 2019; 145(1): 05018002. https://doi.org/10.1061/(ASCE)EY.1943-7897.000058

[26] Javanshir A, Sarunac N. Thermodynamic analysis of a simple Organic Rankine Cycle. Energy. 2017; 118: 85-96. https://doi.org/10.1016/j.energy.2016.12.019

[27] Sami SM. Energy and exergy analysis of new refrigerant mixtures in an organic Rankine cycle for low temperature power generation. Int J Ambient Energy. 2010; 31(1): 23-32. https://doi.org/10.1080/01430750.2010.9675805

[28] Scaccabarozzi R, Tavano M, Invernizzi CM, Martelli E. Comparison of working fluids and cycle optimization for heat recovery ORCs from large internal combustion engines. Energy. 2018; 158: 396-416. https://doi.org/10.1016/j.energy.2018.06.017

[29] Chacartegui R, Sánchez D, Muñoz JM, Sánchez T. Alternative ORC bottoming cycles FOR combined cycle power plants. Appl Energy. 2009; 86(10): 2162-70. https://doi.org/10.1016/j.apenergy. 2009.02.016

[30] Vescovo R, Spagnoli E. High temperature ORC systems. Energy Proc. 2017; 129: 82-9. https://doi.org/10.1016/j.egypro.2017.09.160

[31] Song J, Loo P, Teo J, Markides CN. Thermo-economic optimization of organic Rankine cycle (ORC) systems for geothermal power generation: A comparative study of system configurations. Front Energy Res. 2020; 8: 6. https://doi.org/10.3389/fenrg.2020.00006

[32] Rashwan SS, Dincer I, Mohany A. Analysis and assessment of cascaded closed loop type organic Rankine cycle. Energy Convers Manag. 2019; 184: 416-26. https://doi.org/10. 1016/j.enconman.2018.12.089

[33] Manente G, Lazzaretto A, Bonamico E. Design guidelines for the choice between single and dual pressure layouts in organic Rankine cycle (ORC) systems. Energy 2017; 123: 413-31. https://doi.org/10.1016/j.energy.2017.01.151

[34] Yu X, Geng J, Gao Z. Thermal-economic analysis of an organic rankine cycle system with direct evaporative condenser. J Adv Therm Sci. 2023; 10: 41-58.

[35] Yang H, Xu C, Yang B, Yu X, Zhang Y, Mu Y. Performance analysis of an Organic Rankine Cycle system using evaporative condenser for sewage heat recovery in the petrochemical industry. Energy Convers Manag. 2020; 205: 112402. https://doi.org/10.1016/j.enconman.2019.112402

[36] Marcello S. On the exergoeconomic assessment of employing Kalina cycle for GT-MHR waste heat utilization. Energy Convers Manag. 2015; 90: 364-74. https://doi.org/10.1016/ j.enconman.2014.11.039

[37] Lian Z, Chua K, Chou S. A thermoeconomic analysis of biomass energy for trigeneration. Appl Energy. 2010; 87(1): 84-95. https://doi.org/10.1016/j.apenergy.2009.07.003

[38] Mosaffa AH, Farshi LG, Infante Ferreira CA, Rosen MA. Exergoeconomic and environmental analyses of $CO_2$/$NH_3$ cascade refrigeration systems equipped with different types of flash tank intercoolers. Energy Convers Manag. 2016; 117: 442-53. https://doi.org /10.1016/j.enconman.2016.03.053

[39] Seider WD, Seader JD, Lewin DR, Widagdo S. Product and Process Design Principles: Synthesis, Analysis, and Evaluation, John Wiley; USA: 2004.

[40] Jenkins S. Economic indicators: CEPCI, Chemical Engineering Essentials for the CPI Professional. March 19, 2015. Available from: https://www.chemengonline.com/economic-indicators-cepci/?printmode=1 (Accessed on January 2024).

[41] Pierobon L, Nguyen TV, Larsen U, Haglind F, Elmegaard B. Multi-objective optimization of organic Rankine cycles for waste heat recovery: Application in an offshore platform. Energy. 2013; 58: 538-49.

[42] Turton R, Bailie RC, Whiting WB, Shaeiwitz JA, Bhattacharyya D. Analysis, Synthesis, and Design of Chemical Processes. 4th ed. Pearson Education Inc.; USA: 2009.

[43] Feng Y, Zhang Y, Li B, Yang J, Shi Y. Comparison between regenerative organic Rankine cycle (RORC) and basic organic Rankine cycle (BORC) based on thermoeconomic multi-objective optimization considering exergy efficiency and levelized energy cost (LEC). Energy Convers Manag. 2015; 96: 58-71. https://doi.org/10.1016/j.enconman.2015.02.045

[44] El-Emam RS, Dincer I. Exergy and exergoeconomic analyses and optimization of geothermal organic Rankine cycle. Appl Therm Eng. 2013; 59(1): 435-44. https://doi.org/10.1016/j. applthermaleng.2013.06.005

[45] Sung T, Yun E, Kim HD, Yoon SY, Choi BS, Kim K, *et al*. Performance characteristics of a 200-kW organic Rankine cycle system in a steel processing plant. Appl Energy. 2016; 183: 623-35. https://doi.org/10.1016/j.apenergy.2016.09.018

[46] Thurairaja K, Wijewardane A, Ranasinghe C. Thermo-economic analysis of organic rankine cycle for power generation. In Proceedings of the 2018 IEEE 7th International Conference on Power and Energy (PECon), Kuala Lumpur, Malaysia: 3-4 December 2018; pp. 389-93.

[47] Li T, Zhang Y, Gao H, Gao X, Jin F. Techno-economic-environmental performance of different system configuration for combined heating and power based on organic Rankine cycle and direct/indirect heating. Renew Energy. 2023; 219: 11953. https://doi.org/10.1016 /j.renene.2023.119553

[48] Akman M, Ergin S. Thermo-environmental analysis and performance optimisation of transcritical organic Rankine cycle system for waste heat recovery of a marine diesel engine. Sh. Offshore Struct. 2021; 16(10): 1104-13. https://doi.org/10.1080/17445302. 2020.1816744

[49] Turkan B, Etemoglu AB, Can M. Investigation of thermal architectures for flue-gas assisted organic rankine cycle systems: an assessment for thermodynamics and environmental performance indicators. Energy Sources A: Recovery Util Environ Eff. 2020; 42(4): 505-20. https://doi.org/10.1080/15567036.2019.1587095

[50] Spayde E, Mago PJ, Luck R. Economic, energetic, and environmental performance of a solar powered organic rankine cycle with electric energy storage in different commercial buildings. Energies. 2018; 11(2): 276. https://doi.org/10.3390/en11020276